

Pacific-Australian Plate coupling along New Zealand: determined from velocity calculated by Kostrov summation method

Ying Ting LAU

October 2020



A report submitted in partial fulfilment of the requirements for the degree of Geophysics at Imperial College London and Associateship of the Royal School of Mines. It is substantially the result of my own work except where explicitly indicated in the text. The report may be freely copied and distributed provided the source is explicitly acknowledged.

Word-count: 4727

Abstract

Plate coupling level can be reflected from the discrepancy between the observed plate velocity and the GPS velocity. This study calculated the observed plate velocity of 13 study areas within New Zealand, with 1473 earthquakes recorded between 1976 and 2020 from the Global CMT Catalogue. The observed velocity was compared with GPS velocity provided by GSRM v2.1 (2014) to obtain the regional plate coupling information. Result showed the South Island is highly coupled, with coupling ratio of 0.516-2.481. Stress caused by Australian-Pacific Plate collision was released by seismic processes in form of earthquakes. Whereas plates decoupled along the north, the coupling ratio was decreased by at least one magnitude to 0.002-0.113. The Taupo Volcanic Zone (TVZ) has the lowest seismic coupling. It is believed slow slip events and the heat flow of the region allowed stress released through aseismic processes. The Hikurangi Trench also experienced low seismic coupling. Slow slip earthquakes in the region contributed to the majority of seismic moment release which was not recorded in the Global CMT Catalogue data, resulting to the velocity discrepancy. Slow slip events are concluded as the major reason for the low seismic coupling in the North Island.

Keywords: New Zealand, earthquakes, velocity discrepancy, plate coupling, slow slip earthquakes

1. Introduction

In recent decades, with the technological advancement and joint effort internationally (e.g. cGPS, GSN, NEIC), seismologists have convenient access to moment tensor information of earthquakes online. In this project, we processed earthquake moment tensor data collected by the Global Centroid-Moment-Tensor (CMT) Project and analyzed our study region New Zealand.

Situated at an obliquely converging plate boundary, New Zealand has accumulated a significant amount of stress caused by the friction from the Australian-Pacific Plate collision. (Reyners M., 1998) When stress exceeds the strain of the rock, it breaks and displaces causing earthquakes to occur, while energy is released in form of seismic waves. By measuring the polarity and magnitude of the seismic waves, especially from the first P-wave arrival, we can derive the earthquake's focal mechanism and moment tensor information. (Shearer 2009) We can then calculate the plate velocity (V_{mo}) by using the summed moment tensor of the earthquakes that occurred in the region. (Kostrov 1974) (Detailed calculation can be found later in section 3)

Using the moment tensor summation method for velocity calculation works well

for the southern part of New Zealand, producing velocity within half a magnitude difference to the GPS plate tectonics velocity (V_{GPS}) result. However, moving northward, the velocity discrepancy increases, with a maximum of 2.5 magnitude error in the Taupo Volcanic Zone (TVZ). In TVZ, $V_{mo}=0.113$ mm/year while $V_{GPS}=45.57$ mm/year given by Global Strain Rate Model (GSRM v2.1).

The discrepancy between V_{mo} and V_{GPS} reflects the seismic coupling level of the region. (More details can be found in section 3) High coupling indicates the stress accumulated along the plate boundary at shallow depth (< 50 km in our study area) is released in form of seismic processes like earthquakes. (Beavan J., 2001) Low coupling shows vice versa, stress released through aseismic deformation.

The project aims to calculate the velocity and strain rate using Kostrov summation method and thus deduce the deformation style in different tectonic areas within New Zealand from the plate coupling level. Throughout the project, in each small area, we will find out their 1. Seismic coupling level 2. Deformation style of each region 3. Probability of future earthquake occurrence in the area.

2. Tectonics setting

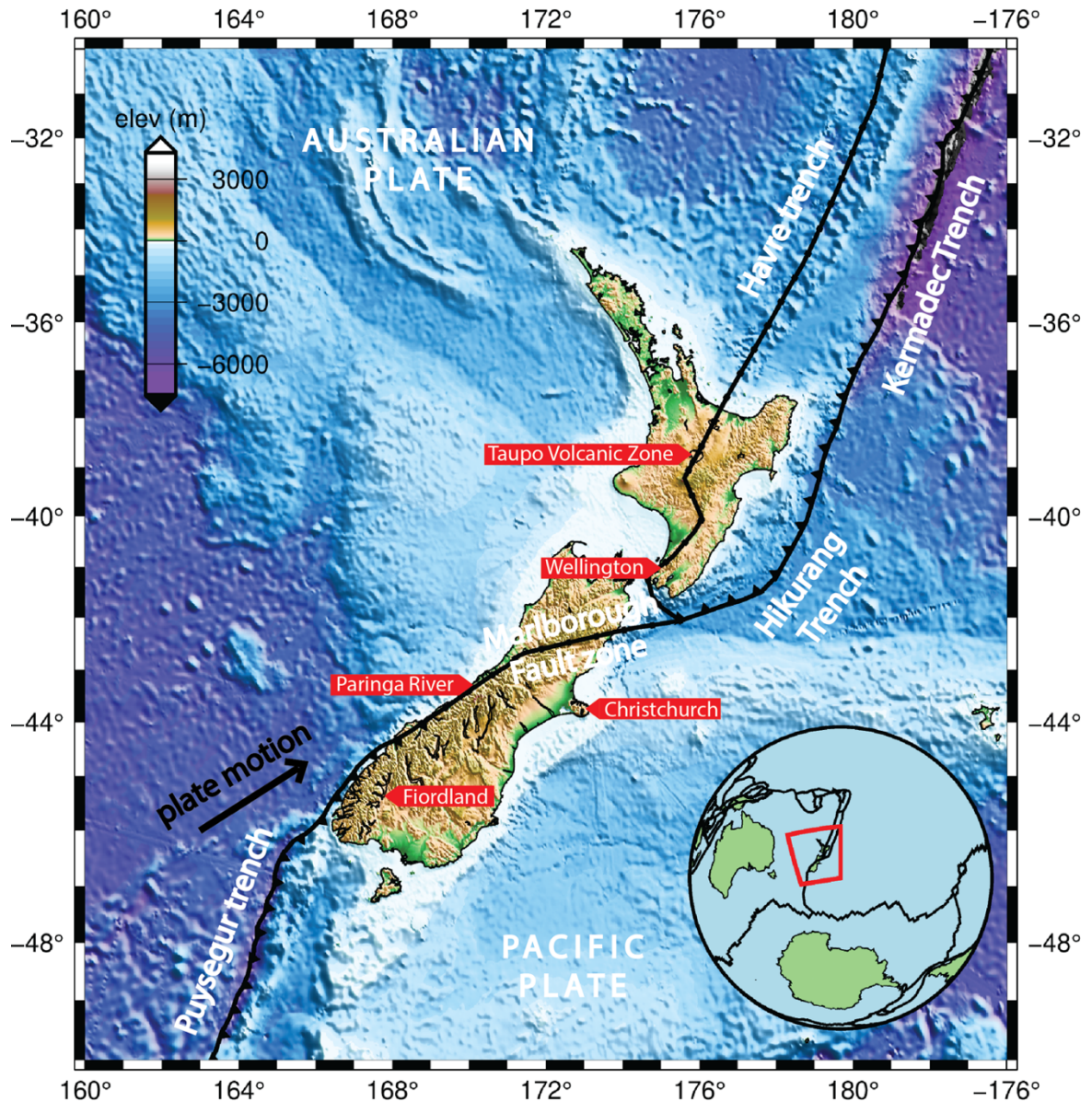


Fig 1. Tectonics setting of New Zealand. Arrow indicates the plate motion of the Australian Plate relative to the Pacific Plate. Dark lines dictate the Australian-Pacific plate boundary, with triangles showing the hanging wall. The Colour scale denotes the topography and bathymetry of the region. Note that the subduction direction is different from Puysegur Trench (south) to Kermadec Trench (north).

New Zealand locates along the Pacific-Australian Plate boundary, with the Australian Plate moving in a north-east direction at around 38 mm/year relative to the Pacific Plate (GSRM v2.1). Along the 2900-km plate boundary in the study area,

we can observe segments of oceanic plate subduction, continental plates collision, transform motion, back-arc rifting, active rotation, and combinations of the above. (e.g. Beavan J. and Haines J., 2001; Lamb S., 2011)

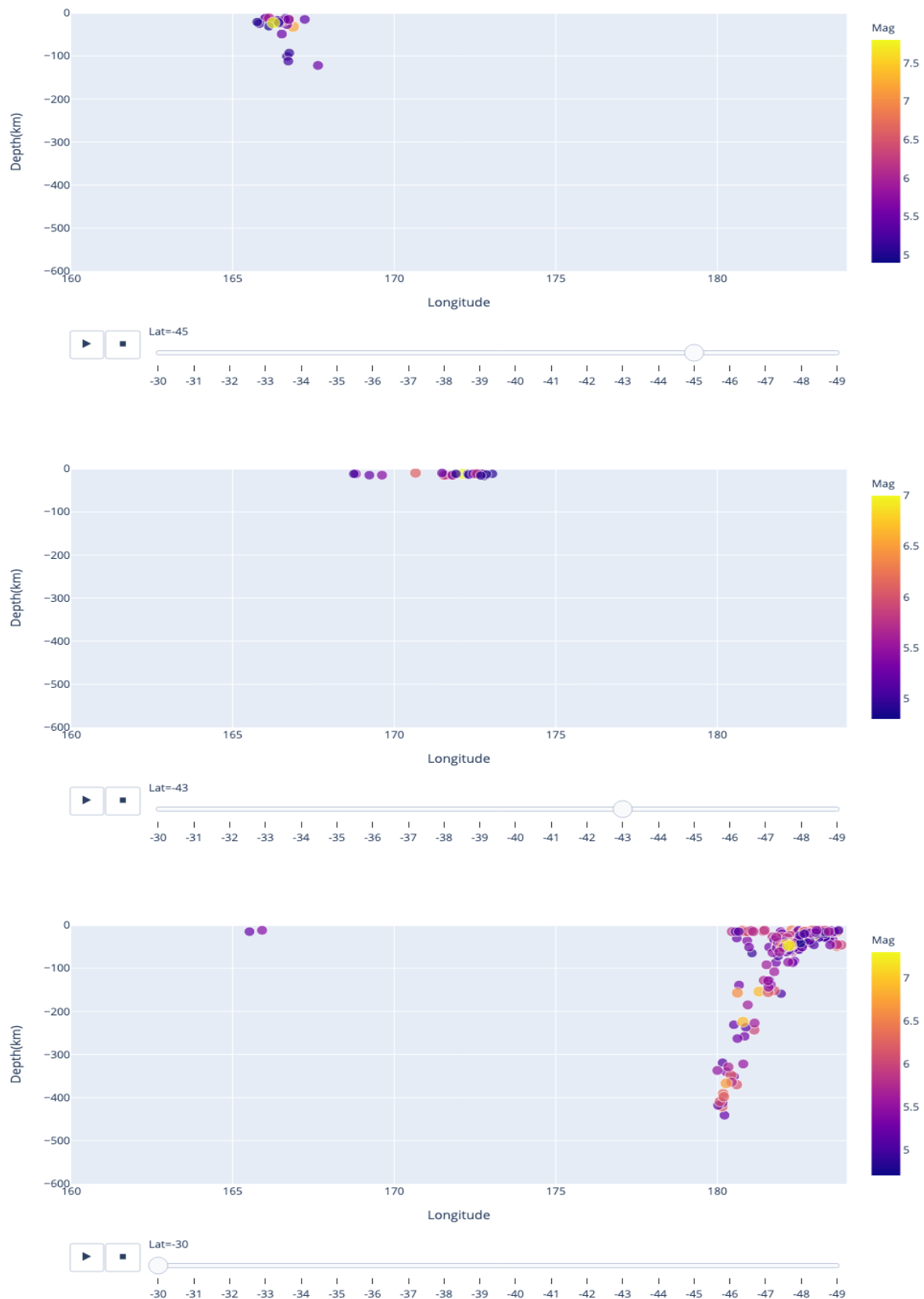


Fig 2. Cross-section slice at latitude -45° (top), -43° (middle), -30° (bottom). The. Each color dot refers to one earthquake. The color bars indicate the moment magnitude (M_w)

In the southwestern water of New Zealand to Fiordland, there lies the Puysegur Trench, where the denser oceanic Australian Plate subducts beneath the buoyant Pacific Plate. The subduction slab is almost vertical when the depth > 40 km (Fig.2 top) and it is relatively shallow subduction terminates at 120 km deep. In this region the crustal seismicity is diffuse. (Anderson, 2001)

Zooming into the South Island, the distinguished Alpine Fault is slicing the land into two-part. The boundary marks a 450-km dextral fault, with up to 100 km of transpression between the lithosphere of two plates and causes uplifting of sedimentary materials, resulting in the rough topography in the Mount Cook National Park near to Paringa River. (Walcott, 1998) The highest uplift rate can be found in the Paringa River, with 13.7 mm/year. (Simpson et al., 1993) In this middle part of New Zealand, minimal subduction occurs. The seismic activities stay in the shallow lithosphere < 15 km (Fig. 2 middle) because the estimated brittle-ductile transition is around 4-12 km depending on the chosen model. (Anderson, 2001)

Move on to the northern part of the South Island, we have the complex Marlborough Fault Zone, where the Alpine Fault separates into four subparallel faults. The

largest fault among all is the Hope Fault. This oblique dextral reverse fault region accommodates 80-100% of the plate motion across the plate boundary zone. (William E., 1995)

In the North Island east water, the subduction direction reversed, with the old and buoyant Pacific Plate changes to oceanic, subducts beneath the continental part of the Australian Plate along the Hikurang-Kermadec Trench. It is assumed that the locked-to-slipped transition interfaced is located beneath Wellington. (Beavan J., 2001) As a result, the lower North Island experienced shallow thrust.

Taupo Volcanic Zone, the middle part of the North Island, has a backarc extension of rate onshore 8-10 mm/year and rotation $2.8^\circ/\text{Myr}$ (Beanland, 1998, Robert A., 2004) Thus, experienced normal faulting in the Taupo region. Note there is a North Island Dextral Fault Belt (NIDFB) in south Taupo to offset the motion of the extension-compression margin. Further east towards the Hikurang Trench, the area experienced backarc spreading and rollback of the Pacific Plate. (Robert A., 2004) This result in the minor constructive movement at the Hikurang Trench region.

North water of New Zealand lies the Kermadec Trench. The Pacific Plate thickness decrease toward the north as less continental feature present. Therefore, the Pacific Plate subduct deeply (> 400 km) under the Kermadec Arc and Australian Plate. (Fig.2 bottom) Dextral motion can be found at the land behind the subduction zone to offset the friction caused by the downgoing slab, forming the Harve Trench. (Kelsey, 1995; Reyners 1998)

3. Methodology

3.1 Seismic coupling

To investigate in plate coupling, we have to first understand the couple mechanism in mechanics. A couple is a system of forces with resultant moment but no net force. (Di-Maggio, 1985) In other words, force couple does not create translation, by having two force of equal magnitude and directed oppositely. In plate coupling terms, one example could be the slab-pull force and friction between plate are coupled, resulting moment. Single couple produces a large torque and causes rotation. Double couple produced no net torque by two couple complementing each other. In a fault system, forces along the fault plane and forces along the auxiliary plan form a double couple. (Fig. 3) There is no net force and net torque on x_1 and x_3 plane.

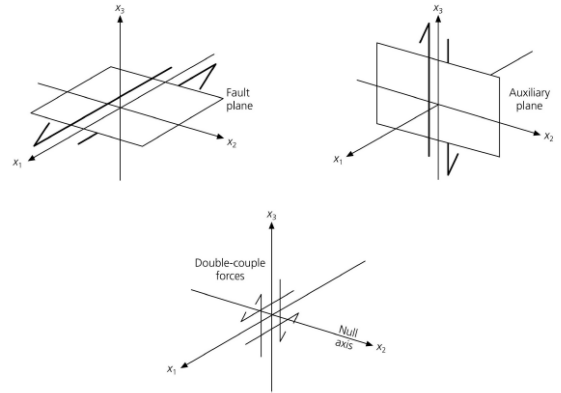


Fig.3 Double couple forces in a fault system
(Pearce, 1997)

Our 3D Earth compose of three planes, each plane contains forces from two opposite directions. As a result, there will be nine force couples composing a seismic moment tensor (M). (Fig. 4)

$$\mathbf{M} = \begin{bmatrix} M_{xx} & M_{xy} & M_{xz} \\ M_{yx} & M_{yy} & M_{yz} \\ M_{zx} & M_{zy} & M_{zz} \end{bmatrix} \quad (3.1)$$

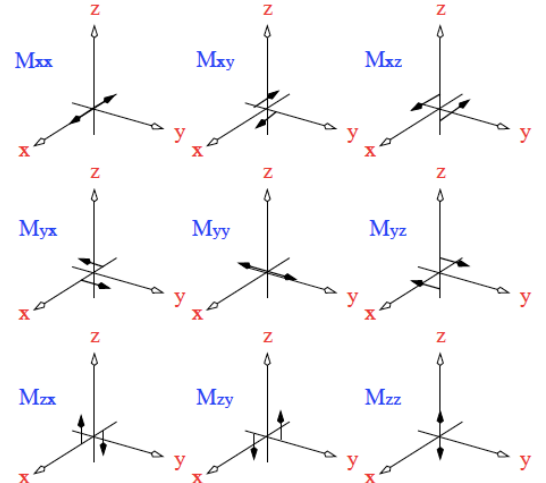


Fig.4 Nine force couples each with net force at the origin equals to zero (Bastow I., 2020)

Due to the conservation of angular momentum, $M_{ij} = M_{ji}$. Therefore, seismic moment tensor has only 6 independent elements, M_{xx} , M_{xy} , M_{xz} , M_{yy} , M_{yz} and M_{zz} . The total seismic moment equals to the sum of the 6 elements.

While the seismic coupling (X_o) is defined as an ratio of observed seismic moment release rate and the rate calculated seismic moment release rate from V_{GPS} . (Scholz C. H., 2012) As the time frame of total observed seismic moment (M_{so}) and calculated seismic moment (M_{TO}) we used are the same, the total moment is used instead of the total moment release rate.

Larger X_o , the plates are more coupled.

$$X_o = M_{so} / M_{TO}. \quad (3.2)$$

In this study, we obtained the earthquake seismic moment tensor data (M_0) and fault plane information from the Global Centroid-Moment-Tensor (CMT) Project, which is useful later for calculating the observed plate velocity (v_{obs}). Through simple summation, M_{so} is obtained. For M_{TO} , we have to derive it from the GPS velocity (v_{GPS}) data using the Kostrov Moment Tensor Summation Method.

3.2 Kostrov Summation Method

Kostrov unprecedently found the relationship between the focal mechanism and seismic moment, and term it the seismic-moment tensor (M_0). M_0 is the characteristic from an earthquake to seismic rock flow (Kostrov, 1972), which is coherent to the observed seismic moment (M_{so}).

Using his method, we can calculate the velocity and strain rate for a volume with known fault length, depth and M_0 . Note that M is limited to the shallow part of the plate prone to brittle deformation. For New Zealand, the brittle deformation depth down to 15 – 50 km depending on the chosen area.

Equation for calculating the regional velocity: (Kostrov, 1972)

$$\text{Velocity} = \frac{1}{\mu L W \tau} \sum_{n=1}^N M_0^n \quad (3.3)$$

Equation for calculating the regional strain rate: (Kostrov, 1972)

$$\frac{d\varepsilon}{dt} = \frac{1}{2\mu V \tau} D_{ij} \quad (3.4)$$

In this project, the length of the earthquake catalogue record (τ) is from January 1976 to October 2020 with seconds as unit; the shear modulus of rigidity (μ) is 3.3×10^{10} Nm⁻²; D_{ij} is the eigenvalues of the summed

M in the region; L is the length of the fault in meter; W is the length of the fault plane in meter; V is the volume of the region. L , W and V are varied in our smaller study areas.

The velocity direction is determined by the fault geometry. For normal faults, the direction equals to the strike of the maximum extensional axis (T-axis). For reverse faults, the direction equals to the strike of the maximum compressional axis (P-axis). For strike-slip faults, the direction is the azimuth of the fault.

Back to M_{TO} , we can compute it using the velocity from GPS data from GSRM v2.1.

$$M_{TO} = \mu L W \tau v_{GPS} \quad (3.5)$$

$$M_{SO} = \mu L W \tau v_{obs} \quad (3.6)$$

As the measurement and the catalogue time is fixed within the same area, we can simply use the GPS velocity and observed velocity to calculate the seismic coupling. Note that the velocity direction has to be calibrated before operation.

$$X_o = v_{obs} / v_{GPS}. \quad (3.7)$$

3.3 Zonation criteria

New Zealand's tectonic varies across the continent. We have divided it into 13 smaller zones to better study the plate coupling and deformation beneath. The zone boundary is determined by the focal mechanism type.

The focal mechanisms in figure 5 is produced by summing up moment tensor M_0 of all earthquakes occurred during the last 44 years and 10 months, and within each 1 degree longitude-latitude zone. Areas without earthquake are exempted. We then grouped areas contain similar focal mechanisms into a small zone for further analysis.

In figure 6, the focal mechanism is plot from the M_0 summation of each zone, producing a distinguish fault geometry, which falls into one of the four categories: normal fault, reverse fault, strike-slip fault and oblique fault.

Calculations and analysis are then conducted specifically for each zone.

3.4 The b-value

After collecting focal mechanism data for, we can compute the moment magnitude (M_w) for each earthquake by a function of M_0 . (Kanamori, 1977)

$$M_w = \frac{2}{3}(\log_{10} M_0 - 9.1) \quad (3.8)$$

Then produce a frequency magnitude plot for earthquakes within the zone. Gutenberg and Richter in 1939 found the relationship between the number of earthquakes (N) and M_w .

$$\log_{10} N = a - bM \quad (3.9)$$

Using the slope, also known as the b-value, we can know the ratio between the large

and small magnitude earthquakes during the catalogue time. The x-intercept of the plot predict the magnitude of the largest earthquake within the earthquake cycle. For New Zealand, the cycle is around 150 years. (Haines, 1995)

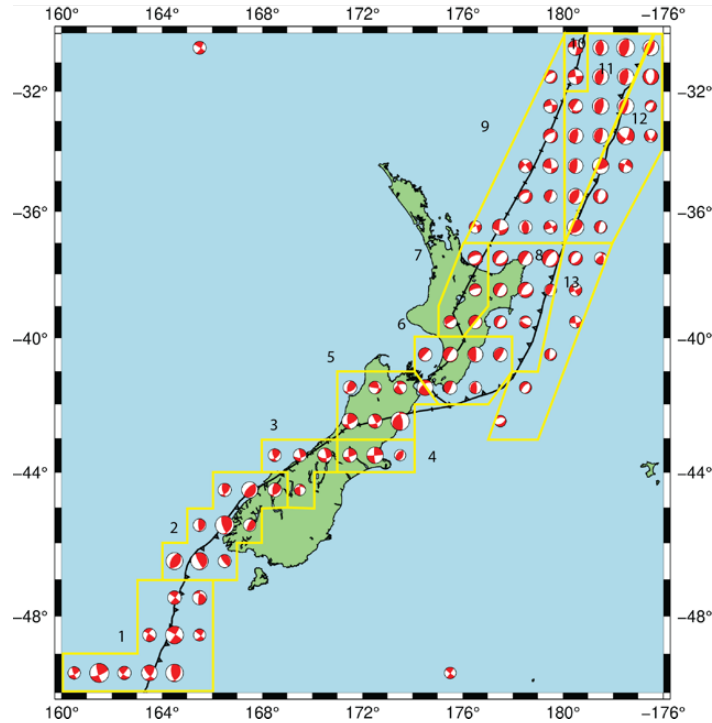


Fig.5 Focal mechanism plot for each 1-degree longitude-latitude region

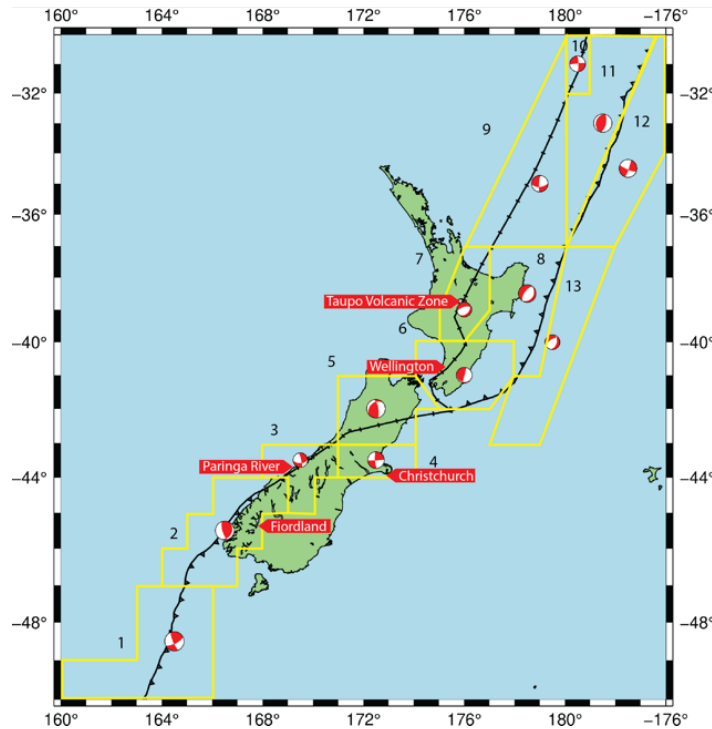


Fig.6 Focal mechanism plot for each zone bounded by yellow line

- | | | |
|---------------------------|---------------------------------------|--------------------------|
| 1. Puysegur Trench | 6. Wellington | 10. Havre Trough (N) |
| 2. Fiordland | 7. Taupo Volcanic Zone | 11. Kermadec Trench (W) |
| 3. Paringa River | 8. Hikurangi Trench (W)/
Raukumara | 12. Kermadec Trench (E) |
| 4. Christchurch | | 13. Hikurangi Trench (E) |
| 5. Marlborough Fault Zone | 9. Havre Trough (S) | |

4. Result and discussion

Table 1. Zone analysis parameters

Zone	Depth (km)	Dip (degree)	v _{obs} (mm/yr)	v _{GPS} (mm/yr)	Direction from N
Puysegur Trench	30	70.65	84.41	34.02	55.24
Fiordland	30	24.9	19.49	37.76	62.49
Paringa River	15	56.28	0.38	39.62	68.59
Christchurch ¹	15	/	/	/	/
Marlborough Fault Zone	25	34.68	34.21	41.03	73.8
Wellington	30	82.33	0.80	41.73	79.1
Taupo Volcanic Zone	30	35.6	0.11	45.57	80.03
Hikurangi Trench (W)/ Raukumara	30	26.85	1.57	45.99	83.35
Havre Trough (S)	50	81.38	0.76	52.57	84.74
Havre Trough (N)	50	83.5	0.75	59.79	86.86
Kermadec Trench (W)	50	63	6.33	56.05	87.71
Kermadec Trench (E) ²	50	/	/	/	/
Hikurangi Trench (E) ³	50	/	/	/	/

¹Christchurch zone does not contain any fault so the velocity and dip cannot be calculated

^{2,3}Assumed Kermadec fault and Hikurangi fault are on the west side, so that velocity and dip cannot be calculated on the trench east

Table 1. (cont.) Zone analysis parameters

Zone	Xo	Strain rate1 (nstrain/yr)	Strain rate2 (nstrain/yr)	b-value	No. of earthquakes
Puysegur Trench	2.481	219	-215	0.53	67
Fiordland	0.516	111	-106	0.58	66
Paringa River	0.010	1.2	-1.4	0.61	6
Christchurch ¹	/	32	-37	0.67	28
Marlborough Fault Zone	0.834	142	-171	0.68	57
Wellington	0.019	1.36	-1.71	0.6	26
Taupo Volcanic Zone	0.002	0.736	-0.715	0.74	35
Hikurangi Trench (W)/ Raukumara	0.034	21	-17	0.68	91
Havre Trough (S)	0.014	1.5	-1.1	0.94	134
Havre Trough (N)	0.013	4.13	-3.96	0.69	63
Kermadec Trench (W)	0.113	26.8	-27.6	0.97	613
Kermadec Trench (E) ²	/	8.35	-8.3	0.94	254
Hikurangi Trench (E) ³	/	0.0998	-0.0586	0.90	16

4.1 South Island

The South Island consists of five study zones, namely Puysegur Trench, Fiordland, Paringa River, Christchurch and the Marlborough Fault Zone. Omit the Paringa region due to change in thermal gradient in the region, X_0 of South Island ranges from 0.516 to 2.481, which shows the Australian Plate and the Pacific Plate are highly coupled. (Figure 7)

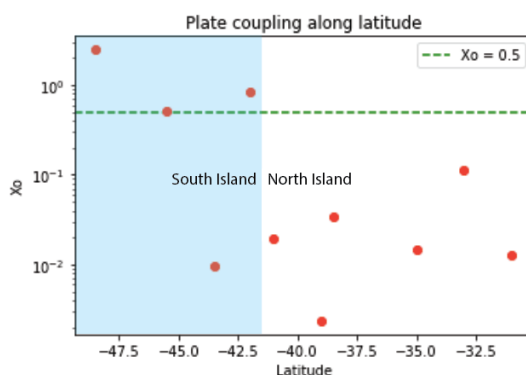


Fig. 7 Plate coupling along latitude plot

Seismicity of the South Island is confine to the crust (Reyners., 1998). 88% of our earthquake data are within 30 km depth. The deeper events are at Puysegur Trench and Southern Alps.

4.1.1 Puysegur Trench

X_0 in this area is the largest among the whole study area, with 2.481. The observed velocity is 84.41 mm/year compared to 34.02 mm/year of GPS velocity. This is a result of high seismic moment of the region. The low b-value (0.53) reflects more large

earthquakes occurred than expected. Crustal seismicity is diffused here. (Leitner et al., 2001) At an oblique compression boundary, stress is easily build up for future rupture. Strain rate perpendicular to the boundary is up to 219 nstrain/year, give rise to high magnitude earthquakes. On the regional frequency magnitude plot, cumulated frequency of $M_w \geq 7.5$ data point does outlay the trendline. (Figure 8)

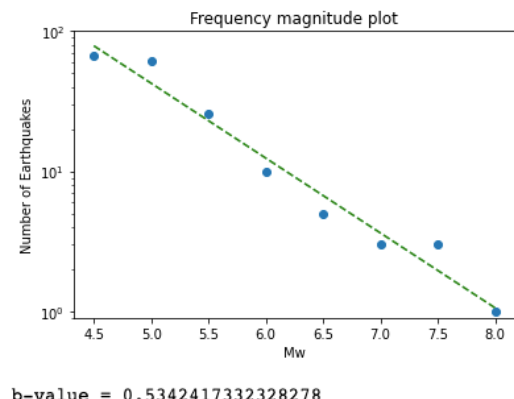


Fig. 8 Puysegur Trench frequency magnitude plot

In fact, there are 3 earthquakes with $M_w > 7$ happened in the last 4 decades causing the velocity discrepancy.

Table 2. Puysegur Trench earthquake data($M_w \geq 7$)

Date	Long	Lat	M_w	M_0
1981/05/25	164.4	-48.9	7.6	$2.74e+27$
2004/12/23	161.3	-49.9	8.1	$1.63e+28$
2007/09/30	164.1	-49.3	7.4	$1.6e+27$

The 2004 earthquake alone produced 10% of the total M_0 of this study region, contributing to the high X_0 . Stress between the Australian-Pacific Plate boundary here

was released in three significant seismic events, proving the plates are highly coupled in this region. The M_w 8.1 earthquake is also the largest earthquake in the whole New Zealand study area, causing Puysegur Trench zone to have a significantly larger v_{obs} compare to other zones.

4.1.2 Fiordland

Fiordland locates at a compressive margin where the Australian Plate's shallow oceanic lithosphere is colliding with the continental lithosphere of the Pacific Plate at 37.76 mm/year. Coupling of the region is moderate, inferring both seismic and aseismic deformation is present in the region. Along the Alpine Fault, density of both lithosphere has a smaller difference than the Puysegur Trench, causing shallow subduction (up to 120 km) and sediment uplifting, elevating the isotherm, forming the Mount Aspiring. Half of the stress between plates is released through seismic rupture along the slab ($X_0 = 0.516$), the other half we suspect it is release through displacement of sediment and heat flow. (more will be discussed in the next section)

4.1.3 Paringa River

This region is not seismically active, only 6 earthquakes are record in the past 44.8 years. Earthquakes are confined in the shallow lithosphere, with no deeper than 15

km. (Table 3) At 4-12 km depth, the brittle-ductile transition zone can be found. (Anderson, 2001) All of the earthquakes are within the transition zone.

Table 3. Paringa River Earthquake data

Date	Long	Lat	Depth(km)	M_w
1984/06/24	170.7	-44.0	10	6.1
1988/05/15	169.2	-43.9	15	5.2
1998/10/20	169.6	-43.8	15	5.4
2005/04/02	170.0	-44.4	12	4.9
2005/05/02	168.8	-43.9	12	5.4
2005/05/02	168.7	-43.9	12	5.0

Despite study shows this region experience transpression up to 100 km (Walcott, 1998), no major earthquakes are found. The highly transpressed Paringa River Area is having the highest uplift rate 13.7mm/year among the whole country. (Simpson et al., 1993) The high uplift rate is connected with a high thermal gradient. Isotherm in this region is elevated by 3-4 km. (Leitner et al., 2001) The recent uplift and erosion history is consistent with a surface temperature gradient of c. 60°C/km. (Allis and Shi, 1995) This high temperature can be reflected by the presence of hot springs and geysers in the region, reflecting surface rocks are having a temperature above 100 °C. Continental uplifting and heat flow (instead of earthquakes) in the region releases stress accumulated at this dextral boundary, resulting a small X_0 (0.01).

4.1.4 Christchurch

Although the Christchurch zone has no plate boundary crossing, several major earthquakes happened in the region. Interestingly, large events ($M_w \geq 6$) only happened within this decade. (Table 4) These large events altered the strain rate of the region by one magnitude. Data from the last three decades result strain rate of 2.44 and -3.35 nstrain/year. Include data of this decade, the strain rate changes to 32 and -37 nstrain/year respectively.

Table 4. Christchurch earthquake data ($M_w \geq 6$)

Date	Long	Lat	M_w	M_0
2010/09/03	172.1	-43.6	7.0	3.64e+26
2011/02/21	162.5	-43.6	6.1	1.86e+25
2011/06/13	162.6	-43.5	6.0	1.09e+25

GPS strain data showed elastic strain accumulation in central South Island is around 20 km southeast to the Alpine Fault. (Beavan et al., 1999) This correlates with a long term strain field of the Christchurch area where no major fault passes through. Yet, located near the junction of the Hope Fault and the Alpine Fault, the local stress field has to be accommodated either by seismic deformation like Earthquake or aseismic deformation such as block rotation or diffuse deformation. (Walcott, 1998) The former option was taken, 2010 earthquake was the result of this long term strain field and causing fault rupture below the surface and the later were smaller aftershocks.

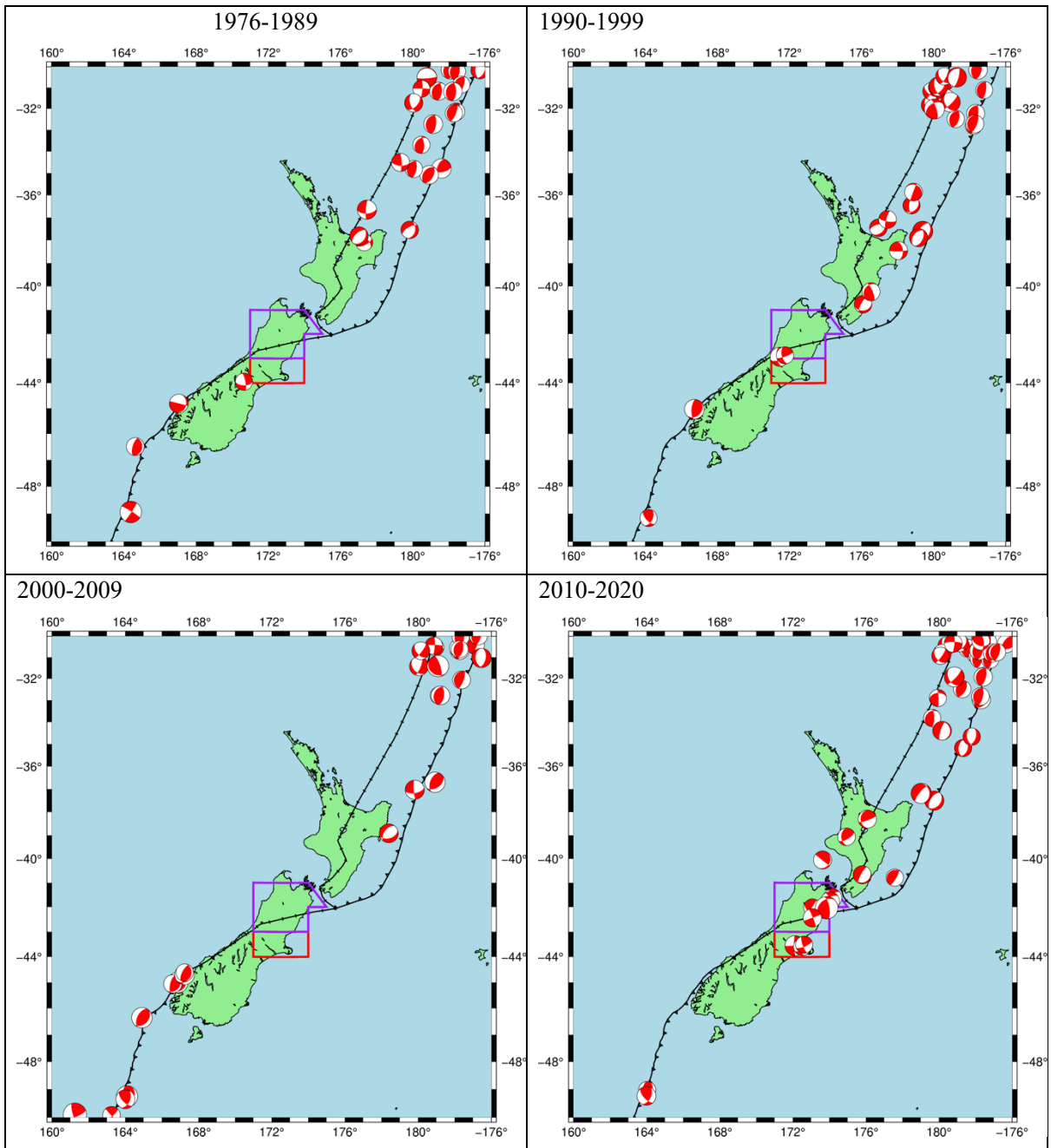


Table 5. Focal mechanism plot of magnitude 6 or above earthquakes.

Red box indicates Christchurch zone and purple box indicates Marlborough Fault Zone

4.1.5 Marlborough Fault Zone

This region is highly coupled with $X_0 = 0.834$, which means stress accumulated within the complex Marlborough Fault Zone is released through seismic rupture. The most active fault among all is the Hope

Fault. The $M_w 6.7$ Earthquake in 1994 and the $M_w 7.8$ Earthquake in 2016 were occurred along the Hope Fault. In the past three decades, similar to the Christchurch region, Marlborough remains tectonically stable. Till this decade, major earthquakes

ruptured. (Table 6) The frequency and intensity are even higher than Christchurch. Data from the last three decades result strain rate of 3.81 and -5.64 nstrain/year. Include data of this decade, the strain rate is increased by 2 magnitude, changes to 142 and -171 nstrain/year respectively. Most of the seismic moment is brought by the 2016 M_w 7.8 earthquake.

Table 6. Marlborough Earthquake data ($M_w \geq 6$)

Date	Long	Lat	M_w	M_0
1994/06/18	171.5	-41.9	6.7	1.45e+26
1995/11/24	171.8	-42.9	6.1	1.8e+25
2013/07/21	174.2	-41.6	6.5	7.0e+25
2013/08/16	174.0	-41.8	6.5	7.78e+25
2015/04/02	173.0	-42.0	6.0	1.24e+25
2016/11/13	173.9	-42.0	7.8	6.7e+27
2016/11/14	173.1	-42.4	6.4	4.74e+25

As the Marlborough Fault Zone region accommodate 80-100% of the plate motion, (Haines J., 2001) large ruptures we encountered in this decade is within expectation. We can also expect one to two more M_w 7 events to happen, to form a complete catalogue.

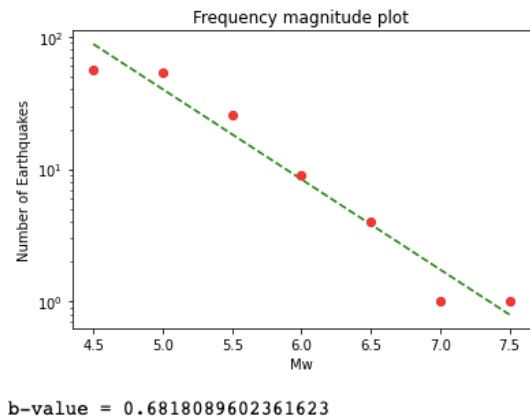


Fig. 9 Marlborough Frequency magnitude plot

4.2 Western North Island

The Western North Island consists of four study zones, namely Wellington, Taupo Volcanic Zone, Havre Trough West and Havre Trough East. X_0 of the Western North Island ranges from 0.002 to 0.019, which shows the Australian Plate and the Pacific Plate are basically decoupled with each other. Stress within plate is released through aseismic processes such as slow slip event (SSE). SSEs are different from earthquakes in terms of their rupture time. SSEs take place over weeks to years, and involve rapid slip along a fault with a rate faster than typical plate motion. (Wallace et al., 2015) Under continuous GPS (cGPS) monitoring, SSEs can be recorded.

4.2.1 Wellington

Wellington locates at a transitional boundary where the Pacific Plate transits from strike-slip motion into subduction. It is assumed that the locked-to-slipped transition interface is located beneath Wellington. (Beavan J., 2001) From figure 6, we can see the focal mechanism of the Wellington zone is a circle divided into half, the western half is red (compression), the eastern counterpart is white (dilatation). This indicates the western continental block is locking the fault and the eastern oceanic plate cannot subduct. The dip of the fault here is 82.33 degree, near vertical, proving a shallow thrust is occurring.

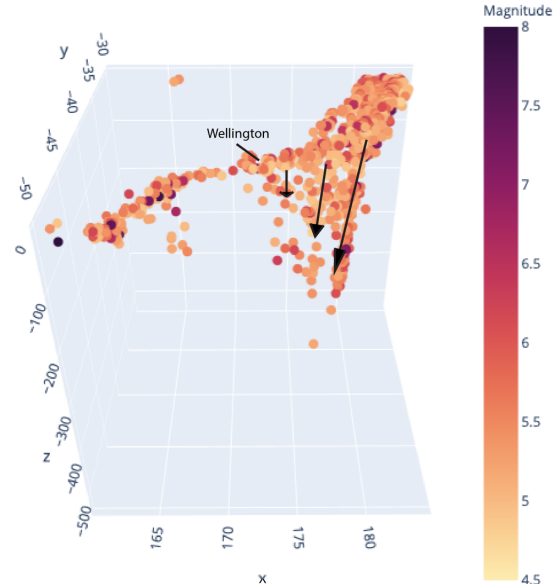


Fig. 10 3D plot showing subduction terminates at Wellington (Arrows indicate the length and direction of the subducting Pacific Plate)

Reyners in 1998 suggested the area is highly coupled due to the observed contraction across the southern North Island. Our data X_0 equals to 0.019 is contrary to his hypothesis. No major earthquakes occurred here ($\text{Max } M_w = 6.4$) despite high stress accumulated during shallow thrust. In fact, the area is highly interseismic coupled. (further explanation in section 4.2.4) Darby and Beanland in 1992 suggest this could be caused by “Slow Earthquake” mechanism. They made a slow slip fault rupture model for the 1855 Wairarapa (in Wellington zone) M_w 8 Earthquake which data fit poorly to the existing models. The Wellington fault has a long term slip rate of 5-8 mm/year. (Van Dissen and Berryman, 1996). This

accommodates aseismic deformation in the compressional region.

4.2.2 Taupo Volcanic Zone (TVZ)

X_0 in TVZ is the smallest among the whole study area, with a value of 0.002, showing the area is decoupled. The v_{obs} is the lowest among the study area, with 0.11 mm/year compare to v_{GPS} of 45.57 mm/year. (Figure 13, 14) In general, the observe plate velocity in the North Island is minimal compare to the South Island.

The cross-section plot of TVZ (figure 11) showed most of the earthquakes are brought by the subducting Pacific Plate. Meanwhile, the shallow lithosphere, <50 km depth is dominated by normal fault. Under normal fault margin, max M_w is usually less than 7 (Hill R., 2008), causing a small M_0 and thus smaller velocity. In our case, the largest M_w we recorded is 6.4.

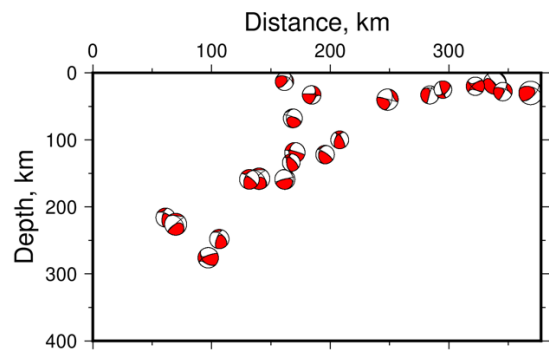
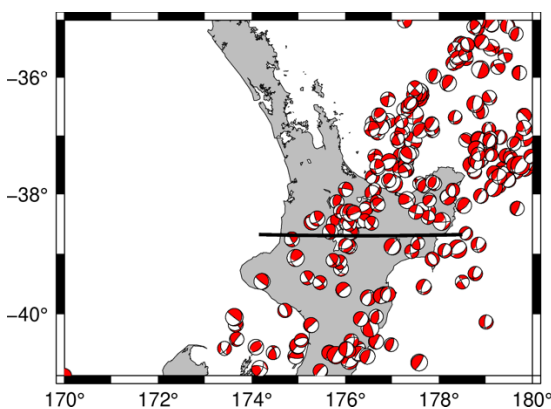


Fig. 11 TVZ cross-section (bottom) indicated by the black line (top)

TVZ is a subaerial region of back-arc rifting. (Haines, 2001) When the Pacific Plate subducts, the partial melt diapirs from the slab up well, causing back-arc rifting in the continent on Australian Plate. Asthenosphere convection continues to drive two side of continental lithosphere apart. The rifting continues and resulting to a volcanic area due to presence of melt and thinning of lithosphere. (Figure 12) Taupo volcano is an active volcano with active hydrothermal venting. (De Ronde, 2002) The volcanicity causes heat flow in the region. Stress can be release in form of heat energy through venting, geysers, hot spring in TVZ. These aseismic processes contribute to plate decoupling.

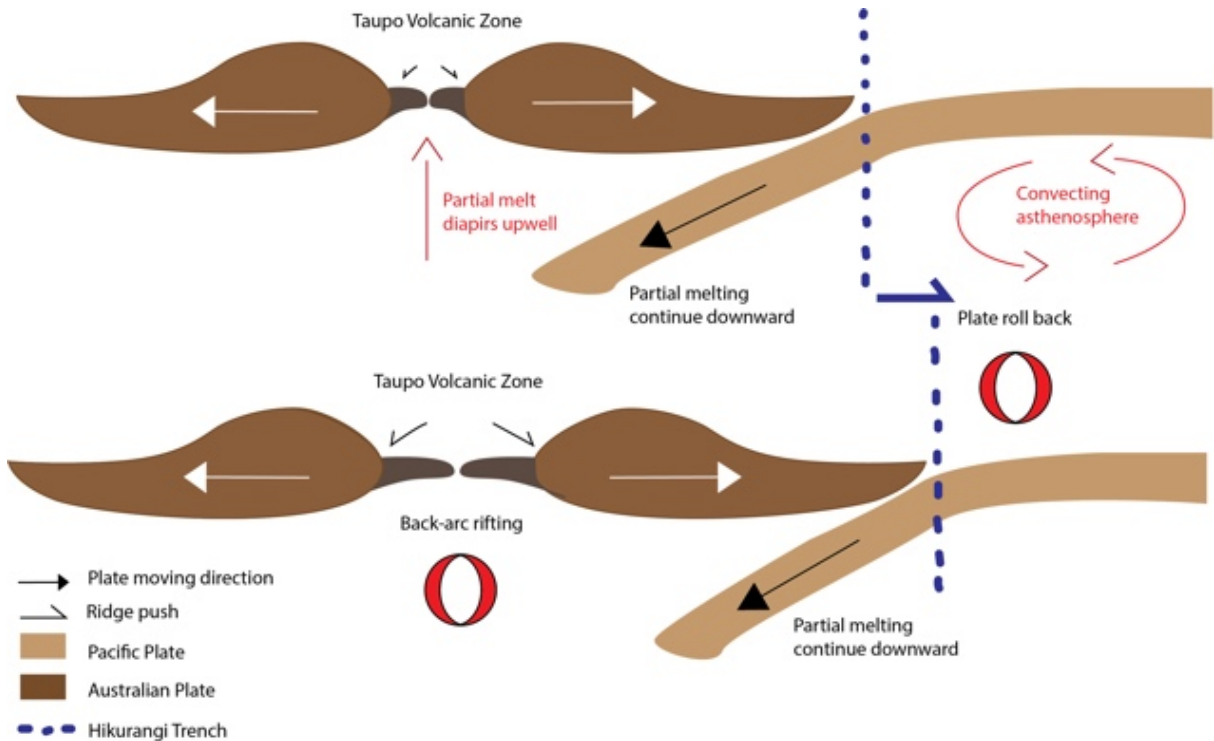


Fig 12. Back arc rifting in TVZ

4.2.3 Havre Trough

The Havre Trough is experiencing low seismic coupling of 0.013-0.014. The dominant motion is dextral sliding, with a nearly vertical dip of $81.38^\circ - 83.5^\circ$. The dextral fault is to accommodate the friction brought by the subducting Pacific slab along the Kermadec Trench. (Rowen and Robert, 2008)

Recent study found there is an early evolution of a young back-arc basin in the Havre Trough. (Tontini, 2019) This can perfectly explain the similarity of X₀ Havre

and TVZ . Geometrically, TVZ and the Havre Trough located on the same ridge where the continent/ seafloor break and spread in the opposite direction. As the back-arc basic of Havre Trough is not mature, the focal mechanism shows it is in an oblique dextral motion.

In the next 3-5 Ma, we could foresee the Havre Trough experiencing more volcanism, creating a volcanic arc and eventually becoming a mature back-arc basin.

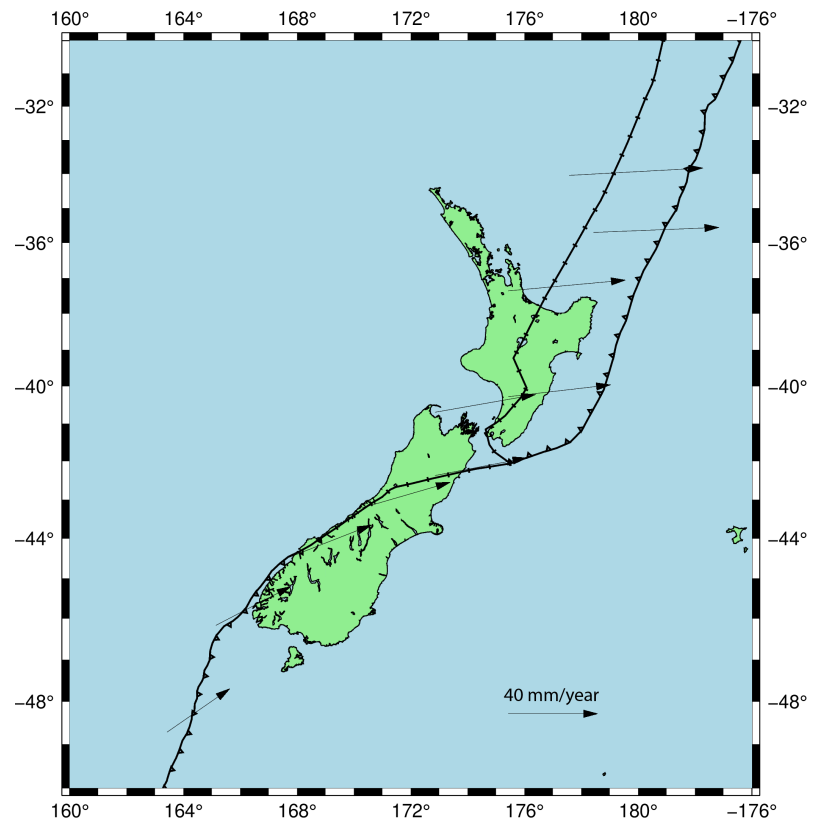


Fig. 13 GPS velocity vector plot

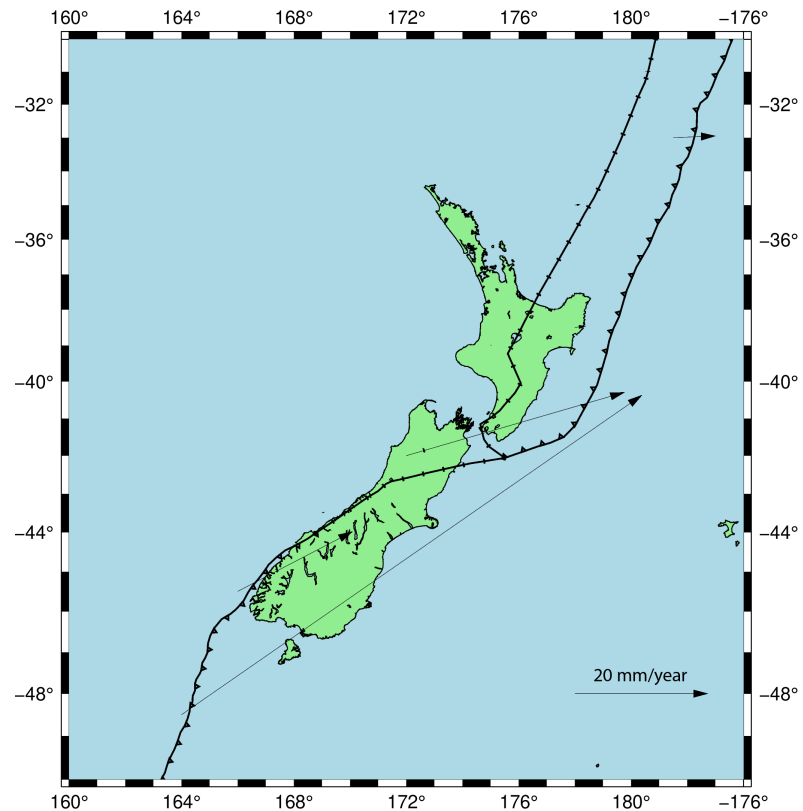


Fig. 14 Observed velocity vector plot

(Velocity arrows in the north are tiny as they are two magnitude smaller than the south)

4.2 Eastern North Island

Pacific Plate transits into a subducting slab in the eastern water of North Island. This changes give rise to all three types of fault geometry, meaning the Hikurangi-Kermadec Trench experiences normal, reverse and transform motion. The Eastern North Island consists of four study zones, namely Raukumara and Hikurangi Trench West, Hikurangi Trench East, Kermadec Trench West and Kermadec Trench East. X_0 of the Hikurangi Trench is 0.034 while the Kermadec Trench is 0.113, showing the Australian Plate and the Pacific Plate are basically decoupled with each other. Stress within plate is released through aseismic processes such as slow slip earthquakes.

4.2.4 Raukumara and Hikurangi Trench West

This is a tectonically interesting area with diverging focal mechanism along a subducting boundary while the plates are highly decoupled ($X_0 = 0.034$). The area, similar to the TVZ, experienced back-arc spreading and rollback of the Pacific Plate.

Most of the study concluded the velocity discrepancy is a result of excluding slow slip events (SSEs) in collecting M_0 . The northern Hikurangi Trench is rich in SSEs. For example, every 18-24 months, Raukumara offshore has a SSE with 1-3 cm

horizontal displacement over 1-2 weeks' time. (Wallace, 2015) In 1947 March, a drop in pressure in the area is recorded by absolute pressure gauge (APG). It was a slow slip tsunami earthquake, proven seismic ruptures can be host by SSEs. (J. Qian et al, 2014)

In this region, we look deeper into the interseismic coupling coefficient, which is the ratio between the interseismic slipping velocity of the fault and the GPS plate velocity. (Metois, M, 2016) As the Pacific Plate subduction gradually locked at the Wellington Area (see figure 10), the Hikurangi forearc experienced clockwise rotation. It was rotated clockwise by $80^\circ - 90^\circ$ in the past 20 Ma, averagely $4^\circ - 4.5^\circ$ per Myr. (Lamb S., 2011) The rotation today resulted in shallow thrust at Wellington and difference plate converging rate along northern (~ 60 mm/year) and southern (~ 20 mm/year) Hikurangi Trench. (Wallace, 2004) Thus, the slip deficit rate is different along latitude. (figure 15) It is concluded that the southern Hikurangi is more interseismic coupled than the northern side, overall Hikurangi has high interseismic coupling level (0.7-0.8). Oppositely, the northern side is more seismic coupled ($X_0 = 0.034$) than the southern end ($X_0 = 0.019$), the value are both low, but the north is more

likely to occur an earthquake than the south, even though the area is dominated by SSEs.

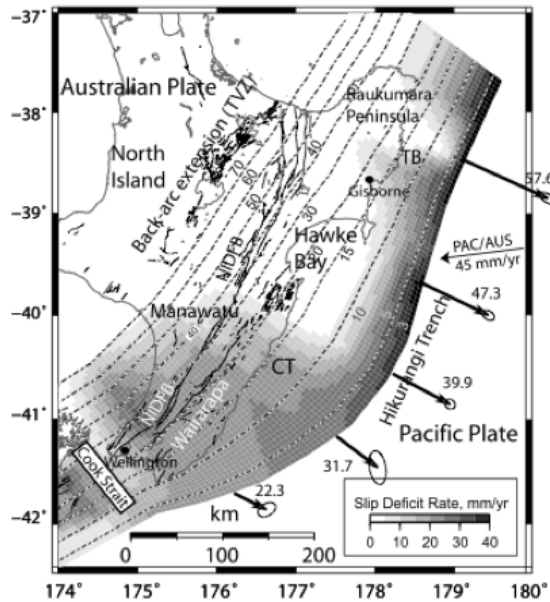


Fig. 15 Hikurangi Trench West interseismic coupling (in terms of slip deficit rate)

(from Wallace et al., 2009a)

Wallace in 2010 further summarise the characteristic of SSEs in Hikurangi. Largest SSEs occur in the southern part, with longer duration and deeper in the fault (around 40 km), while smaller SSEs happens in the northern part with shorter duration and shallower depth.

Other than SSEs, thick sediment also account for the low X_o . Reyners in 1998 found out a narrow zone of high P-wave to S-wave velocity along the fault and suggested an elevated fluid pressure from subducted sediment is causing it. Presence of thick sediment could result in

underestimating the seismic moment of the measured earthquakes. Thus resulting a smaller X_o than the reality.

4.2.5 Hikurangi Trench East

Despite the zone area is 93000 sq. km, it experienced only 16 earthquakes in the past 4 decades, with the highest M_w as 5.8. Stress in the region are released in form of SSEs along the trench. Within 2002 and 2010, 15 SSEs have been recorded by cGPS along the Hikurangi Trench. (Wallace, 2010) Most seismic and aseismic activities occur on the west side of the trench due to the westward dipping subduction slab, where friction is build up.

The roll back of Pacific Plate due to convection cell of the asthenosphere turn this region into a constructive plate boundary. (Figure 14) Smaller M_w can be found in this type of boundary and release less seismic moment during small earthquakes, thus creating low coupling.

4.2.6 Kermadec Trench West

Seismic activities are highly active in this region with 613 earthquakes recorded in 44.8 years' time. From figure 16, we can conclude the seismic deformation pattern is coherent, 95% of focal mechanisms indicates reverse fault.

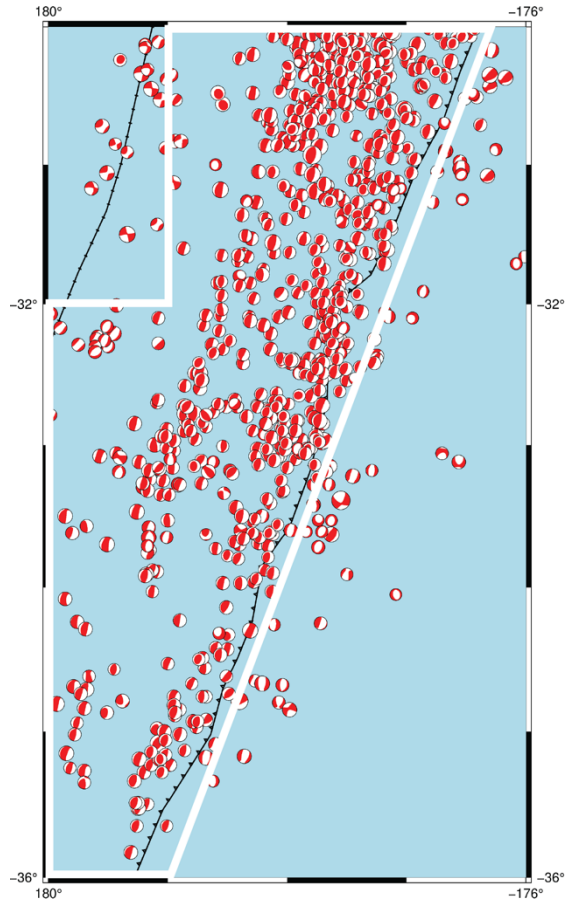


Fig. 16 Kermadec trench west focal mechanisms
(White box bounds the Kermadec West Zone)

Although significant amount of seismic moment was released through earthquakes, v_{obs} is 8.85 times smaller than v_{GPS} . This is to say majority of the stress built up in the region is release through aseismic means,

resulting the low plate coupling. (Figure 17) As the deepest earthquake in the region is 528 km deep, we can imagine the transitional zone is proportionally lengthen.

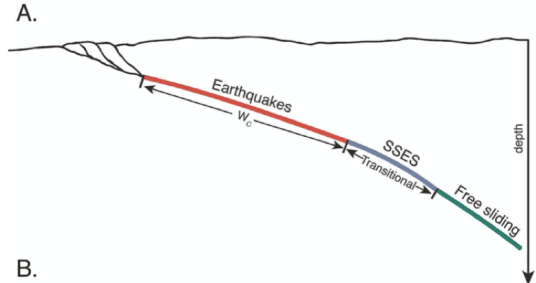


Fig. 17 Subduction zone with Earthquakes and SSEs (from Scholz and Campos, 2011)

4.2.7 Kermadec Trench East

Opposite to the west counterpart, Kermadec Trench has a variety of deformation style, resulting in a sinistral pattern. Number of earthquakes in the east trench is 3 times less than the west, indicating stress within subduction zone is mainly release on the west trench as the slab is dipping toward the west. (see figure 2 bottom)

5. Error analysis

In this section we will discuss the short coming of analysing plate coupling using the Kostrov Summation Method and listing errors which affect the value of our parameters.

5.1 Variable accuracy

Our analysis rely on v_{obs} value. Recall equation 3.3:

$$\text{Velocity} = \frac{1}{\mu LWT} \sum_{n=1}^N M_0^n \quad (3.3)$$

v_{obs} is depending on 5 variables, μ , τ , L , W and M_0 . The μ we used equals to 3.3×10^{10} . However, shear modulus changes upon the rock type. Generally, volcanic and metamorphic rocks have higher μ up to 3.6×10^{10} . For volcanic region like TVZ, velocity could be smaller in reality. The L and W are estimated to have 20% of error, as the fault itself is not a straight line passing through two coordinates. The τ is a constant 44 years and 10 months. Lastly, M_0 is related to the problem of sparse sampling. It is dominated by the few largest event. (Scholz and Campos, 2012) From the Christchurch zone, three events in two years altered its M_0 by 1.5 magnitude. Put aside M_0 , the maximum velocity error is 48%.

5.2 Sensitivity analysis

M_0 value is obtained secondarily from the Global CMT Project. The accuracy depends vastly on the sensitivity of seismic stations. Also, the data date back to 1976, in which the equipment is less proficient. We can expect less small M_w earthquakes are detected back in those days. As a result, the frequency of low M_w is smaller than expected. (Figure 18) However, as mentioned in the previous section, M_0 is dominated by large earthquakes. The absence of small earthquakes does not bring a major error.

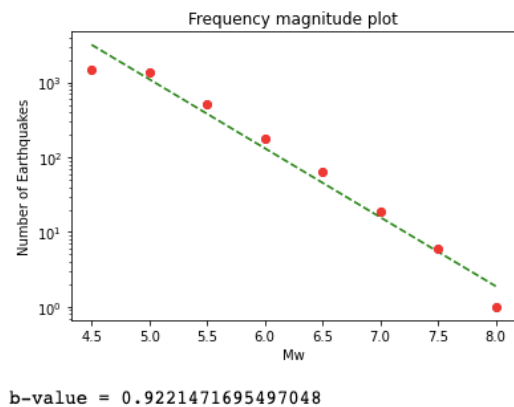


Fig. 18 Frequency magnitude plot of the whole study area

5.3 Catalogue completeness

A complete catalogue should sample all earthquakes within a earthquake cycle, which is around 200-300 year for New Zealand supported by Paleoseismic Evidence. (Leiter et.al, 2001; Bull and Brandon, 1998) New Zealand is in a co-seismic phrase which large earthquakes happened within the past 4 decades,

especially in the south where b-value is small. (Figure 19) From figure 18, we can tell the area's catalogue is close to complete.

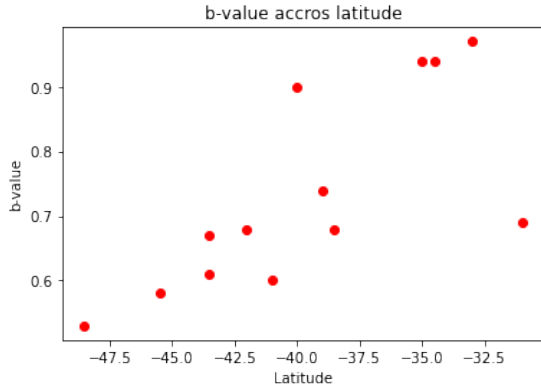


Fig. 19 b-value across latitude

5.4 Dispersion

The earth is a low-pass filter, which the low frequency component of the wave remain. The seismic wave experiences attenuation before arriving the station. Attenuation can be caused by geometric spreading, absorption and scattering. (Sanchez-Salinero, 1986) The degree of attenuation depends on the geology of rocks the wave passes through.

6. Conclusion

We have analysed the plate coupling mechanism throughout New Zealand. It is concluded that the level of seismic coupling decrease northward, with TVZ having the lowest level of plate coupling. In the South Island, stress within plate boundary is mainly released through earthquakes. Except from Paringa River Region, where the isotherm is elevated, with aseismic deformation dominated in form of heat flow. The b-value of the southern zones are smaller, indicating there are more high magnitude earthquakes than expected. Especially in the Marlborough and Christchurch region where the Alpine Fault is separate into parallel sub-fault. Meanwhile, in the Northern Island, stress

are released through aseismic deformation.

The X_0 in here is 1-2 magnitude smaller than the southern counterpart. In the Hikurangi region, slow slip events are a common way of removing friction. In TVZ and Havre Trough, heat flow is an useful mean to remove stress in form of heat energy.

In the past 4 decades, major earthquakes with $M_w > 7$ occur in New Zealand, completing the catalogue. It is concluded the area entered the end of co-seismic stage. We could expect at most 1-2 more large earthquakes and the earthquake cycle here will back to a new starting point.

Acknowledgements

This work was supported by Imperial College London. I have greatly benefited by many discussion with my course coordinator Dr. Ian Bastow whose expertise in earthquake seismology. He advised me with a research direction in aseismic deformation , particularly slow slip earthquake in the region. Gratitude also goes to Rita Kounoudis, Edward P. Andrews, Tom Merry, Catherine Spurin, Evelyn Baker and Edward Caunt. They all provided me with invaluable guidance and coding support essential to the project completion. An important part of database obtained for this project was from Global CMT Catalogue Search, which is updated and maintained by G. Ekström and M. Nettles. Their unsung effort provided valuable data for this project.

Reference

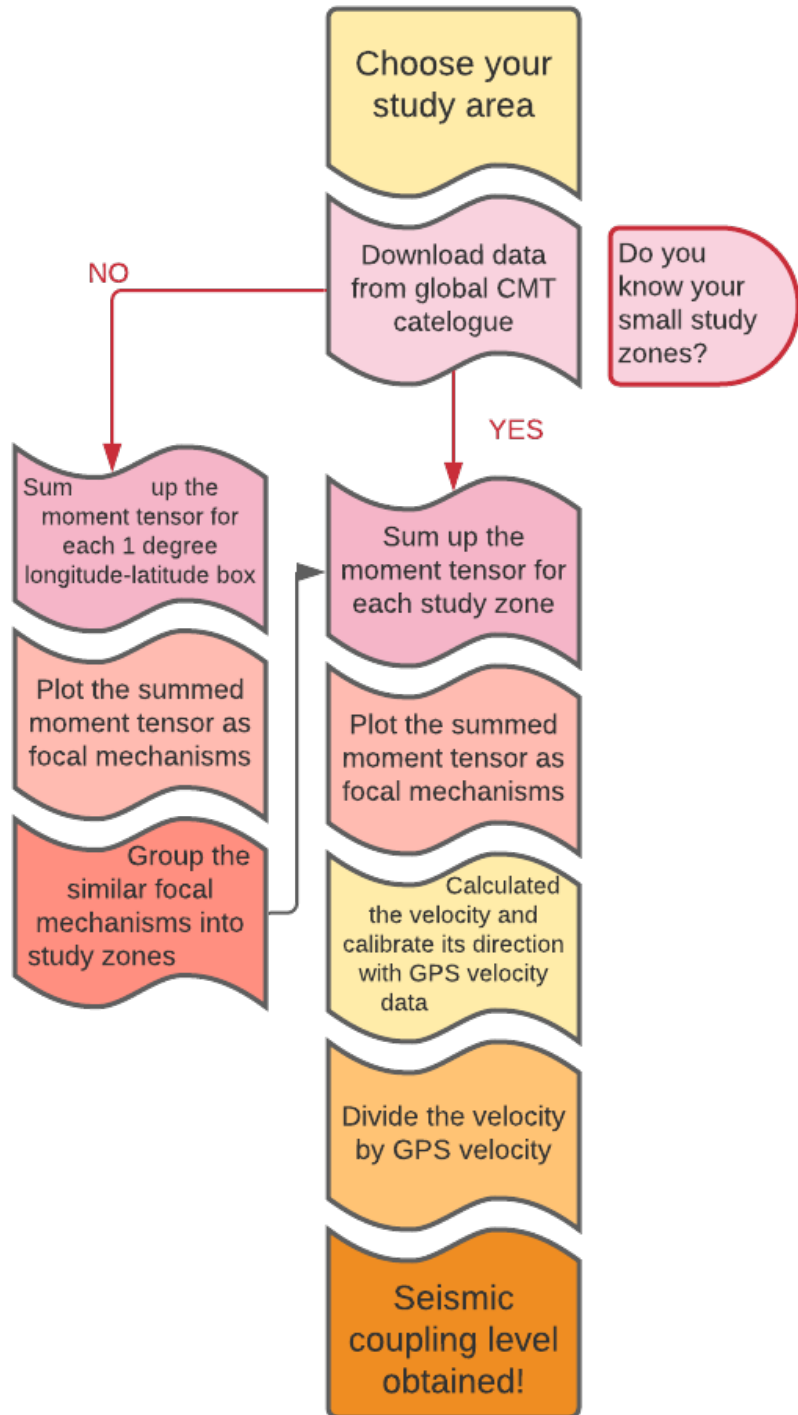
- Allis, R.G. and Shi, Y., 1995. New insights to temperature and pressure beneath the central Southern Alps, New Zealand. *New Zealand journal of geology and geophysics*, 38(4), pp.585-592.
- Allmann, B.P. and Shearer, P.M., 2009. Global variations of stress drop for moderate to large earthquakes. *Journal of Geophysical Research: Solid Earth*, 114(B1).
- Bastow, I., 2020. Independent Geophysics Course Materials. Imperial College London.
- Beavan, J. and Haines, J., 2001. Contemporary horizontal velocity and strain rate fields of the Pacific-Australian plate boundary zone through New Zealand. *Journal of Geophysical Research: Solid Earth*, 106(B1), pp.741-770.
- Beanland, S. and Haines, J., 1998. The kinematics of active deformation in the North Island, New Zealand, determined from geological strain rates. *New Zealand Journal of Geology and Geophysics*, 41(4), pp.311-323.
- Bull, W.B. and Brandon, M.T., 1998. Lichen dating of earthquake-generated regional rockfall events, Southern Alps, New Zealand. *Geological Society of America Bulletin*, 110(1), pp.60-84.
- Darby, D.J. and Beanland, S., 1992. Possible source models for the 1855 Wairarapa earthquake, New Zealand. *Journal of Geophysical Research: Solid Earth*, 97(B9), pp.12375-12389.
- De Ronde, C.E.J., Stoffers, P., Garbe-Schönberg, D., Christenson, B.W., Jones, B., Manconi, R., Browne, P.R.L., Hissmann, K., Botz, R., Davy, B.W. and Schmitt, M., 2002. Discovery of active hydrothermal venting in Lake Taupo, New Zealand. *Journal of Volcanology and Geothermal Research*, 115(3-4), pp.257-275.
- DiMaggio, F.L., 1986. Dynamics: Theory and applications: by TR Kane and DA Levinson, McGraw-Hill, New York, 1985, xv+ 379 pp.
- Hillis, R.R., Sandiford, M., Reynolds, S.D. and Quigley, M.C., 2008. Present-day stresses, seismicity and Neogene-to-Recent tectonics of Australia's 'passive' margins: intraplate deformation controlled by plate

- boundary forces. Geological Society, London, Special Publications, 306(1), pp.71-90.
- Holt, W.E. and Haines, A.J., 1995. The kinematics of northern South Island, New Zealand, determined from geologic strain rates. *Journal of Geophysical Research: Solid Earth*, 100(B9), pp.17991-18010.
- Kanamori, H., 1977. The energy release in great earthquakes. *Journal of geophysical research*, 82(20), pp.2981-2987.
- Kelsey, H.M., Cashman, S.M., Beanland, S. and Berryman, K.R., 1995. Structural evolution along the inner forearc of the obliquely convergent Hikurangi margin, New Zealand. *Tectonics*, 14(1), pp.1-18.
- Kostrov, V.V., 1974. Seismic moment and energy of earthquakes, and seismic flow of rock. *Izv. Acad. Sci. USSR Phys. Solid Earth*, Engl. Transl., 1, pp.23-44.
- Lamb, S., 2011. Cenozoic tectonic evolution of the New Zealand plate-boundary zone: A paleomagnetic perspective. *Tectonophysics*, 509(3-4), pp.135-164.
- Leitner, B., Eberhart-Phillips, D., Anderson, H. and Nabelek, J.L., 2001. A focused look at the Alpine fault, New Zealand: Seismicity, focal mechanisms, and stress observations. *Journal of Geophysical Research: Solid Earth*, 106(B2), pp.2193-2220.
- Metois, M., Vigny, C. and Socquet, A., 2016. Interseismic coupling, megathrust earthquakes and seismic swarms along the Chilean subduction zone (38–18 S). *Pure and Applied Geophysics*, 173(5), pp.1431-1449.
- Pearce, R. (1977), Fault plane solutions using relative amplitudes of P and pP, *Geophys. J. R. Astr. Soc.*, 50(2), 381–394.
- Reyners, M., 1998. Plate coupling and the hazard of large subduction thrust earthquakes at the Hikurangi subduction zone, New Zealand. *New Zealand Journal of Geology and Geophysics*, 41(4), pp.343-354.
- Rowan, C.J. and Roberts, A.P., 2004. Rotation of the Hikurangi Margin, East Coast, New Zealand: Reconciling Long-Term Deformation Patterns Indicated by Paleomagnetic and Magnetic Fabric Data With the Short-Term Velocity Field. AGU FM, 2004, pp.GP43A-0842.
- Sanchez-Salinero, I., Roessel, J.M., Stokoe, I.I. and Kenneth, H., 1986. Analytical studies of body wave propagation and attenuation. TEXAS UNIV AT AUSTIN GEOTECHNICAL ENGINEERING CENTER.
- Scholz, C.H. and Campos, J., 2012. The seismic coupling of subduction zones revisited. *Journal of Geophysical Research: Solid Earth*, 117(B5).
- Simpson, G.D., Cooper, A.F. and Norris, R.J., 1994. Late quaternary evolution of the Alpine fault zone at Paringa, South Westland, New Zealand. *New Zealand journal of geology and geophysics*, 37(1), pp.49-58.
- Tontini, F.C., Bassett, D., de Ronde, C.E., Timm, C. and Wysoczanski, R., 2019. Early evolution of a young back-arc basin in the Havre Trough. *Nature Geoscience*, 12(10), pp.856-862.
- Van Dissen, R.J. and Berryman, K.R., 1996. Surface rupture earthquakes over the last~1000 years in the Wellington region, New Zealand, and implications for ground shaking hazard. *Journal of Geophysical*

- Research: Solid Earth, 101(B3), pp.5999-6019.
- Walcott, R.I., 1998. Modes of oblique compression: Late Cenozoic tectonics of the South Island of New Zealand. *Reviews of geophysics*, 36(1), pp.1-26.
- Wallace, L.M. and Beavan, J., 2010. Diverse slow slip behavior at the Hikurangi subduction margin, New Zealand. *Journal of Geophysical Research: Solid Earth*, 115(B12).
- Wallace, L.M., Webb, S.C., Ito, Y., Mochizuki, K., Hino, R., Henrys, S., Schwartz, S.Y. and Sheehan, A.F., 2016. Slow slip near the trench at the Hikurangi subduction zone, New Zealand. *Science*, 352(6286), pp.701-704.
- Wallace, L.M., 2020. Slow slip events in New Zealand. *Annual Review of Earth and Planetary Sciences*, 48, pp.175-203.

Appendix I

Flow-chart of calculating the seismic coupling level for the study area



Appendix II

Content of Electronic supplementary material

The zip file contains of 4 directories and 1 README.txt file. Please read the README.txt for more instructions.

Directory 1 – Python code

large zone (North-east).ipynb
large zone (North-west).ipynb
large zone (South).ipynb
Moment tensor.ipynb
Plate analysis.ipynb
Plotly.ipynb
Shapely.ipynb
Small grid.ipynb
Smallzonegrp.ipynb
Zone 1 analysis.ipynb
Zone 10 analysis.ipynb
Zone 11 analysis.ipynb
Zone 12 analysis.ipynb
Zone 13 analysis.ipynb
Zone 2 analysis.ipynb
Zone 3 analysis.ipynb
Zone 4 analysis.ipynb
Zone 5 analysis.ipynb
Zone 6 analysis.ipynb
Zone 7 analysis.ipynb
Zone 8 analysis.ipynb
Zone 9 analysis.ipynb

Directory 2 – GMT code

~\$rain and velocity plot.docx

bird_plates.xy
NZ_all.gmt
NZ_CMT5_1990199.gmt
NZ_CMT5_20002009.gmt
NZ_CMT5_20102019.gmt
NZ_CMT6_19762020.gmt
NZ_CMT6_19801989.gmt
NZ_CMT6_19901999.gmt
NZ_CMT6_20002009.gmt
NZ_CMT6_20102019.gmt
NZ_full.gmt
NZ_globe.gmt
NZ_SUM.gmt
NZ_trial.gmt
Strain and velocity plot.docx
tiral.gmt
Tomography.grd

Directory 3 – Excel spread sheets

Data.xlsx
Summary.xlsx

Directory 4 – Data

GPS_DATA.txt
location.txt
meca70.txt
meca70m.txt
meca70mag.txt
NZ_all_m0.txt
NZ_all_m0mw.txt

NZ_all.txt	NZ_map.txt
NZ_CMT5_19901999.txt	NZ_trial.txt
NZ_CMT5_20002009.txt	plate data.xlsx
NZ_CMT5_20102019.txt	smallzonegrp.txt
NZ_CMT6_19762020.txt	smallzonegrpall.txt
NZ_CMT6_19801989.txt	SUM.txt
NZ_CMT6_19901999.txt	TT_data.txt
NZ_CMT6_20002009.txt	
NZ_CMT6_20102019.txt	
.	